PHYSICAL REVIEW LETTERS **128,** 072501 (2022)

Precise Measurement of Differential Cross Sections of the $\Sigma^- p \rightarrow \Lambda n$ Reaction in Momentum Range 470–650 MeV/c

K. Miwa,[1] J. K. Ahn,[2] Y. Akazawa,[3] T. Aramaki,[1] S. Ashikaga,[4] S. Callier,[5] N. Chiga,[1] S. W. Choi,[2] H. Ekawa,[6] P. Evtoukhovitch,[7] N. Fujioka,[1] M. Fujita,[8] T. Gogami,[4] T. Harada,[4] S. Hasegawa,[8] S. H. Hayakawa,[1] R. Honda,[3] S. Hoshino,[9] K. Hosomi,[8] M. Ichikawa,[4,14] Y. Ichikawa,[8] M. Ieiri,[3] M. Ikeda,[1] K. Imai,[8] Y. Ishikawa,[1] S. Ishimoto,[3] W. S. Jung,[2] S. Kajikawa,[1] H. Kanauchi,[1] H. Kanda,[10] T. Kitaoka,[1] B. M. Kang,[2] H. Kawai,[11] S. H. Kim,[2] K. Kobayashi,[9] T. Koike,[1] K. Matsuda,[1] Y. Matsumoto,[1] S. Nagao,[1] R. Nagatomi,[9] Y. Nakada,[9] M. Nakagawa,[6] I. Nakamura,[3] T. Nanamura,[4,8] M. Naruki,[4] S. Ozawa,[1] L. Raux,[5] T. G. Rogers,[1] A. Sakaguchi,[9] T. Sakao,[1] H. Sako,[8] S. Sato,[8] T. Shiozaki,[1] K. Shirotori,[10] K. N. Suzuki,[4] S. Suzuki,[3] M. Tabata,[11] C. d. L. Taille,[5] H. Takahashi,[3] T. Takahashi,[3] T. N. Takahashi,[15] H. Tamura,[1,8] M. Tanaka,[3] K. Tanida,[8] Z. Tsamalaidze,[7,12] M. Ukai,[3,1] H. Umetsu,[1] S. Wada,[1] T. O. Yamamoto,[8] J. Yoshida,[1] and K. Yoshimura[13]

(J-PARC E40 Collaboration)

Contents

1. Introduction (1)

Motivation

・Hyperon-Nucleon (YN) interaction are fundamental information for describing nuclear systems such as hypernuclei and neutron stars.

・To understand the strong interaction in the nonperturbative region

Importance of $\Sigma^- + p \to \Lambda + n$

The strength of $\Sigma N - \Lambda N$ coupling is related to the hyperon puzzle in neutron stars.

- To constrain the strength of the two body $\Sigma N - \Lambda N$ coupling, reactions involving the conversion such as $\Sigma^- + p \to \Lambda + n$ are important.

1. Introduction (2)

Recently Experimental Research

・Accurate measurement of $\frac{d\sigma}{d\Omega}$ of the $\Sigma^{-}p$ elastic scattering in the momentum ($p_{\Sigma^{-}_{incident}}$) range $470 - 850$ MeV/c (the J-PARC E40) —> the P and higher-wave interactions

・Updated total cross section of the Λp elastic scattering for $0.9 \le p_{\Lambda} \le 2.0$ GeV/c (the CLAS collaboration)

—> the S wave interaction

・Particle correlation for YN and YY pairs (the ALICE and STAAR collaboration)

Theoretical frameworks of BB interactions

- Lattice QCD

Used in this paper

- the chiral effective field theory (χEFT)
- Nijmegen models (Effective Soft-Core model) (ESC08c, ESC16)

  ↕

  Hard-Core ($r \to r_c$, $V \to +\infty$)
- fss2

⋮

1. Introduction (4)

Reaction used for this experiment

$\pi^- + p \to \Sigma^- + K^+$ (Σ^- produces)

$\Sigma^- + p \to \Lambda + n$ (Secondary reaction)

$\downarrow$

$p + \pi^-$ (Λ decay)

Back ground reactions

(1) $\Sigma^- + p \to \Sigma^- + p$ (elastic scattering)

$\downarrow$

$\pi^- + n$

(2) $\Sigma^- + p \to \Sigma^0 + n$

$\downarrow$

$\gamma + \Lambda$

$\searrow p + \pi^-$

(3) $\Sigma^- \to \pi^- + n$ (Σ^- decay)

$\pi^- + p \to \pi^- + p$ or $n + p \to n + p$ (elastic scattering)

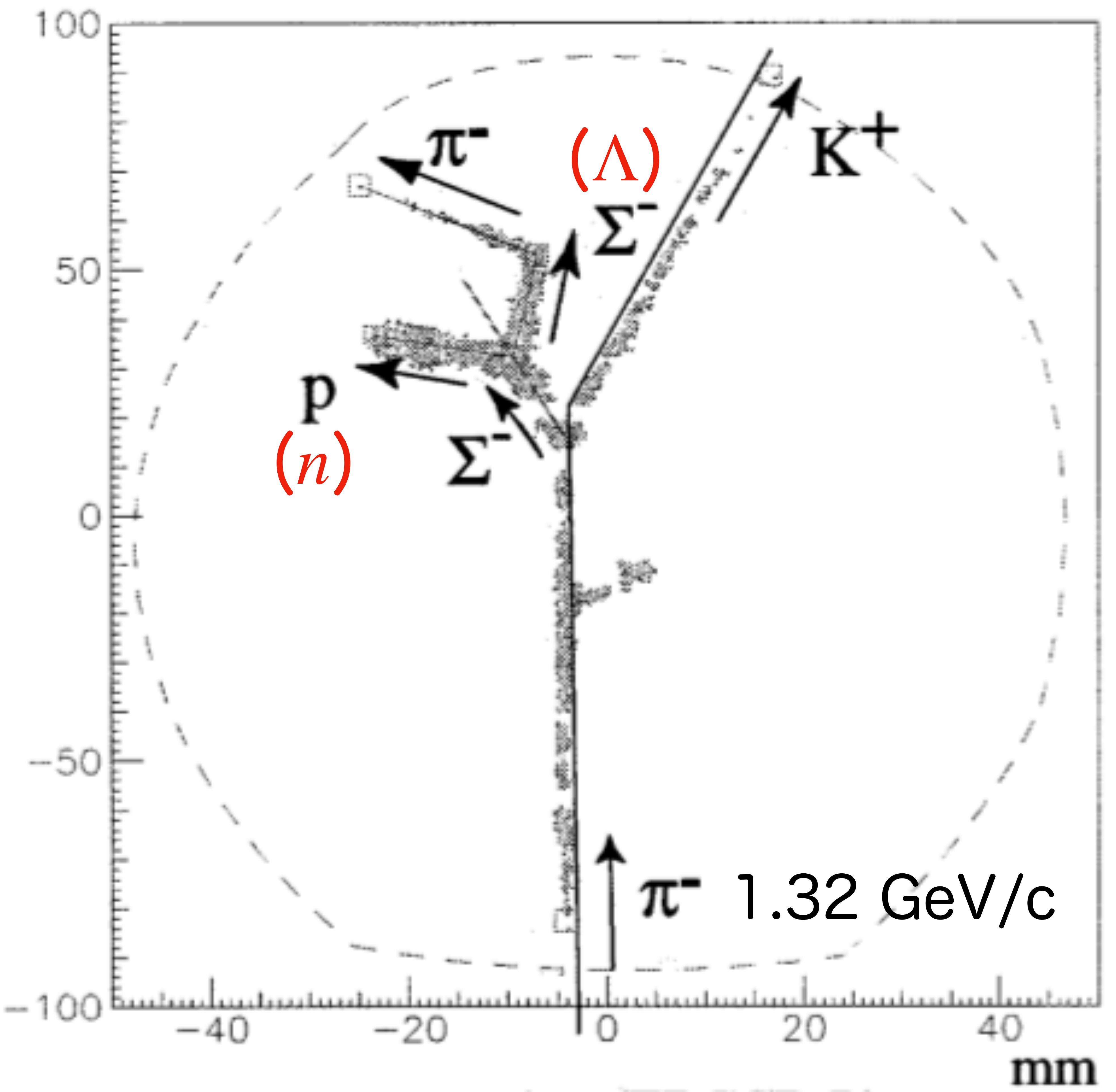

Y.Kondo et al, Nucl. Phys. A676, 371 (2000)

K2 beam line of the 12GeV KEK-Proton Synchrotron (E251)

2. Experiment

J-PARC K1.8

1.33 GeV/c π^- beam 2.0×10^7 /spill

Cycle of 5.2 sec & beam duration of 2 sec

Total 1.62×10^7 Σ^- particles were used.

Σ^- momentum —> missing momentum
(with an ccuracy of 5 MeV/c)

Secondary reaction (e.g. $\Sigma^- + p \rightarrow \Lambda + n$) were identified kinematically from the charged particles in the final state using CATCH system.

PID between π^- and p —> $dE - E$ method

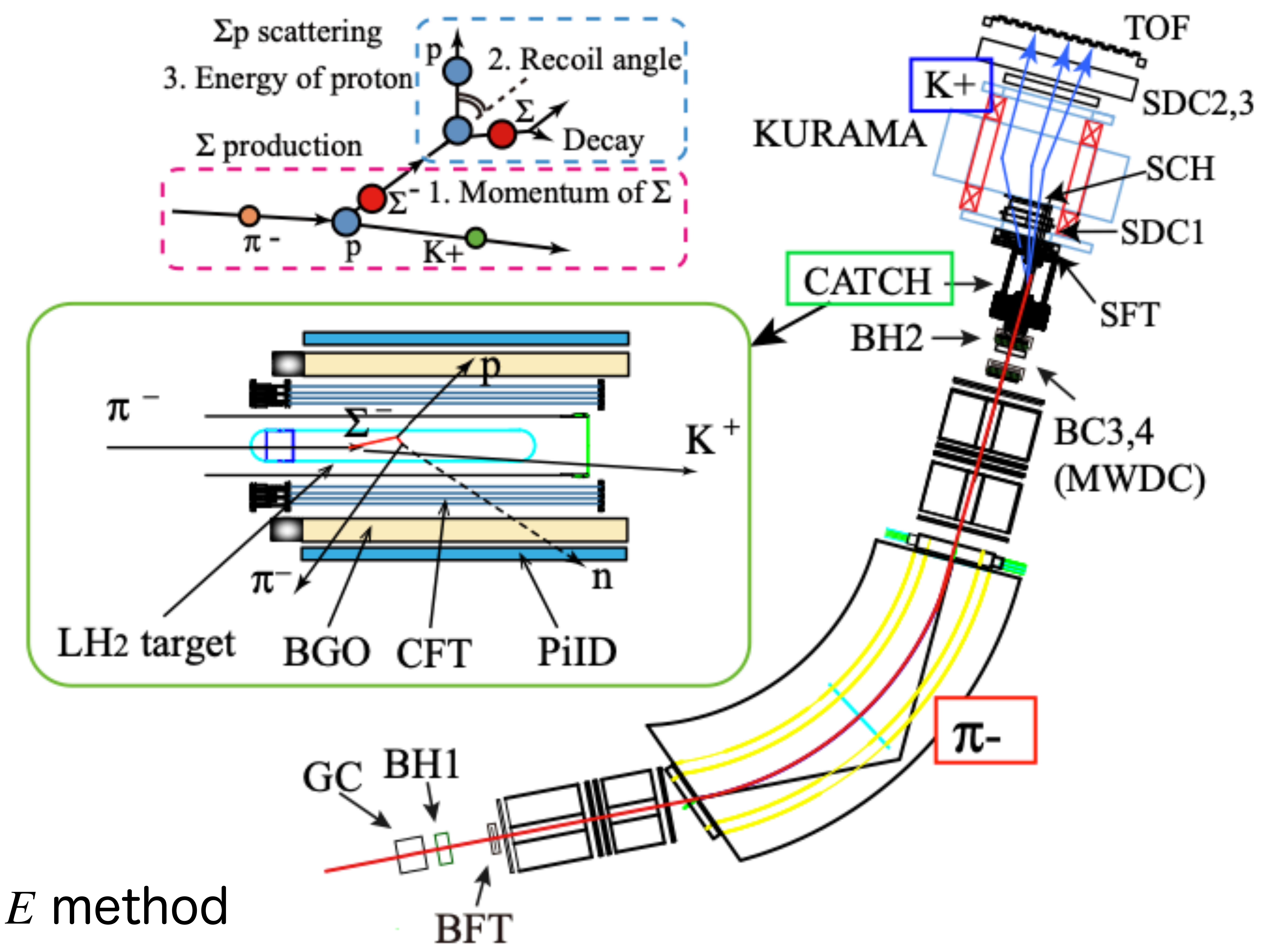

・The E_{kin} of p and direction of p and π^- were measured using CATCH.

・p_π was determined such that m_π and m_p became m_Λ (using p_p and the opening angle the two tracks).

3. Analysis (1)

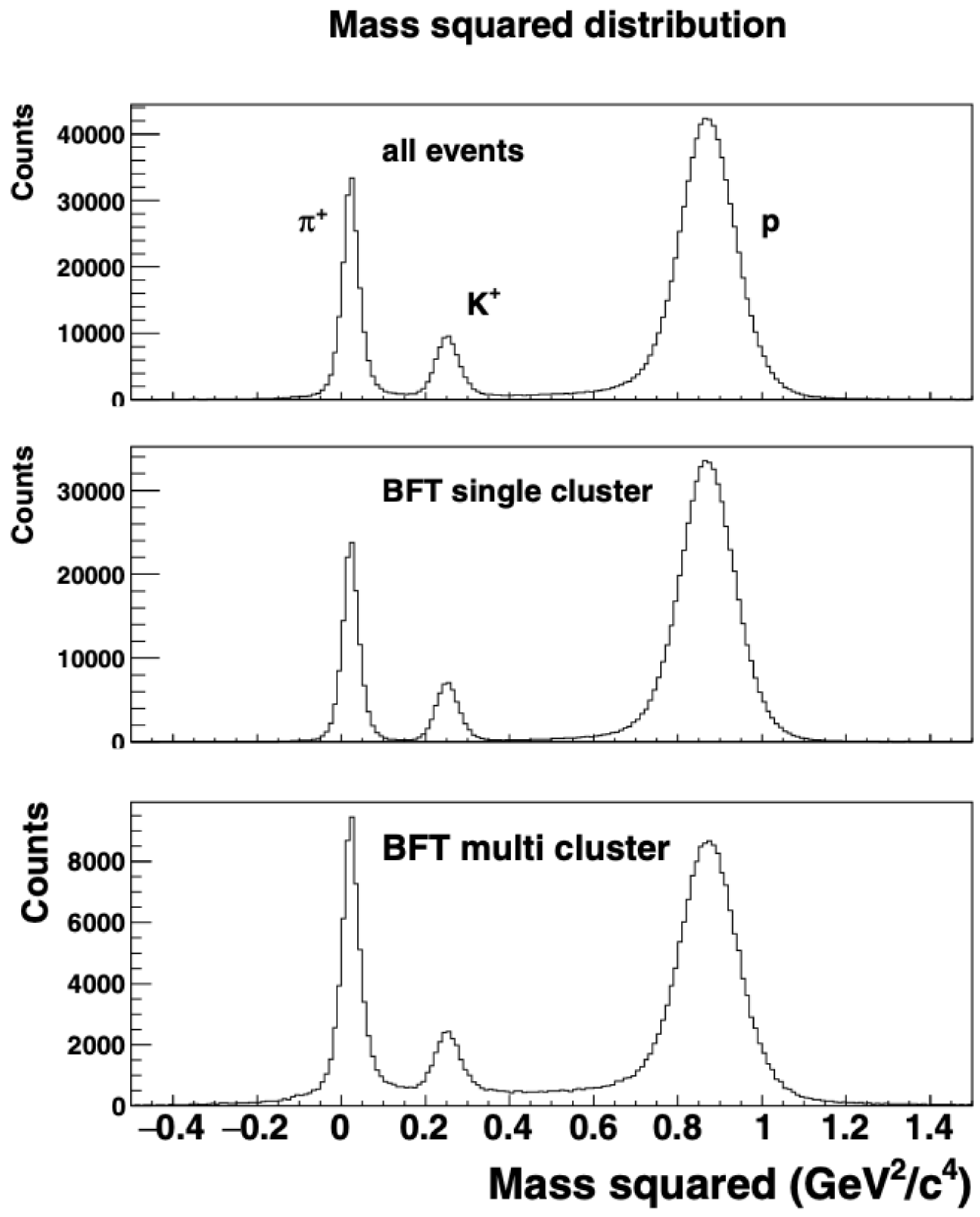

FIG. 3. Reconstructed mass squared distribution for all events (top), BFT single cluster events (middle), and BFT multicluster event (bottom).

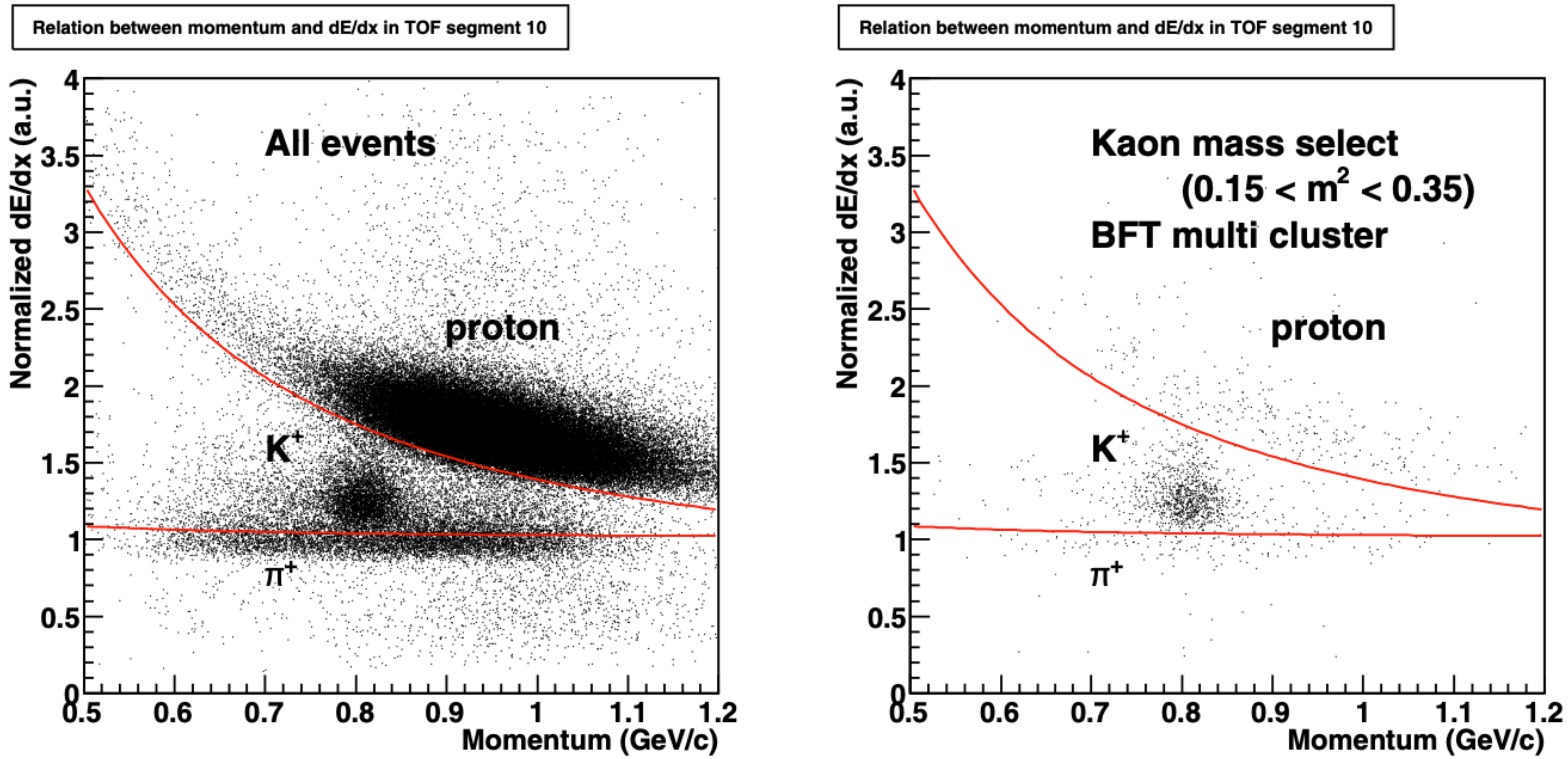

FIG. 4. Correlation between the momentum and energy deposit per unit length at the TOF, which was normalized as one for π^+. Left and right figures show the correlations of all events and the K^+ mass region for the BFT multicluster event, respectively. The region between two red lines was selected as the K^+ region for the BFT multicluster event.

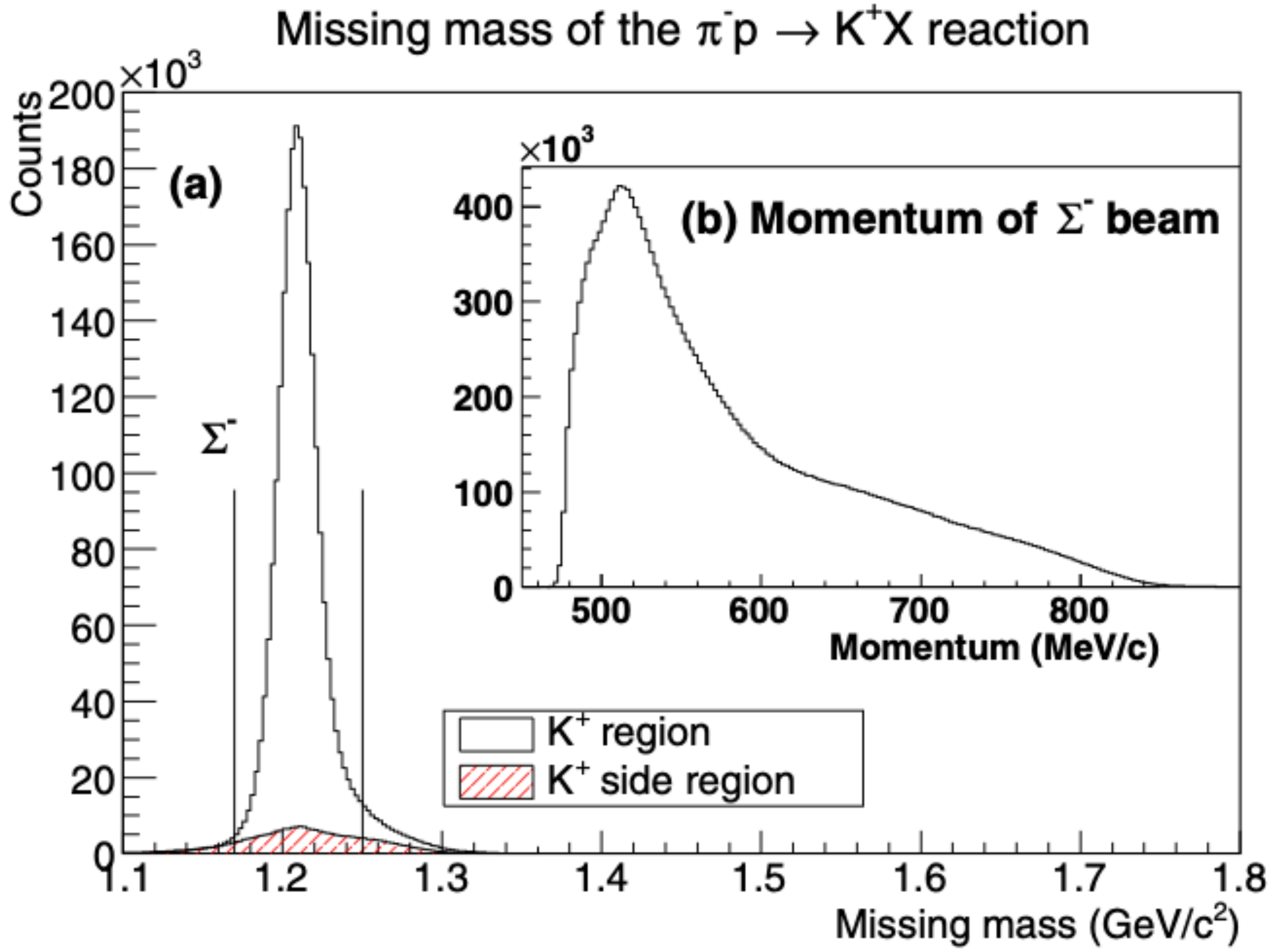

FIG. 6. (a) Missing mass spectra of the $\pi^- p \to K^+ X$ reaction for K^+ events (open histogram) and sideband events of K^+ (filled histogram) to estimate the effect of the contamination of the miscalculated event under the K^+ region in the mass square spectrum. The two lines show the selected area for the Σ^- particles. (b) Σ^- momentum reconstructed as the missing momentum of the $\pi^- p \to K^+ \Sigma^-$ reaction.

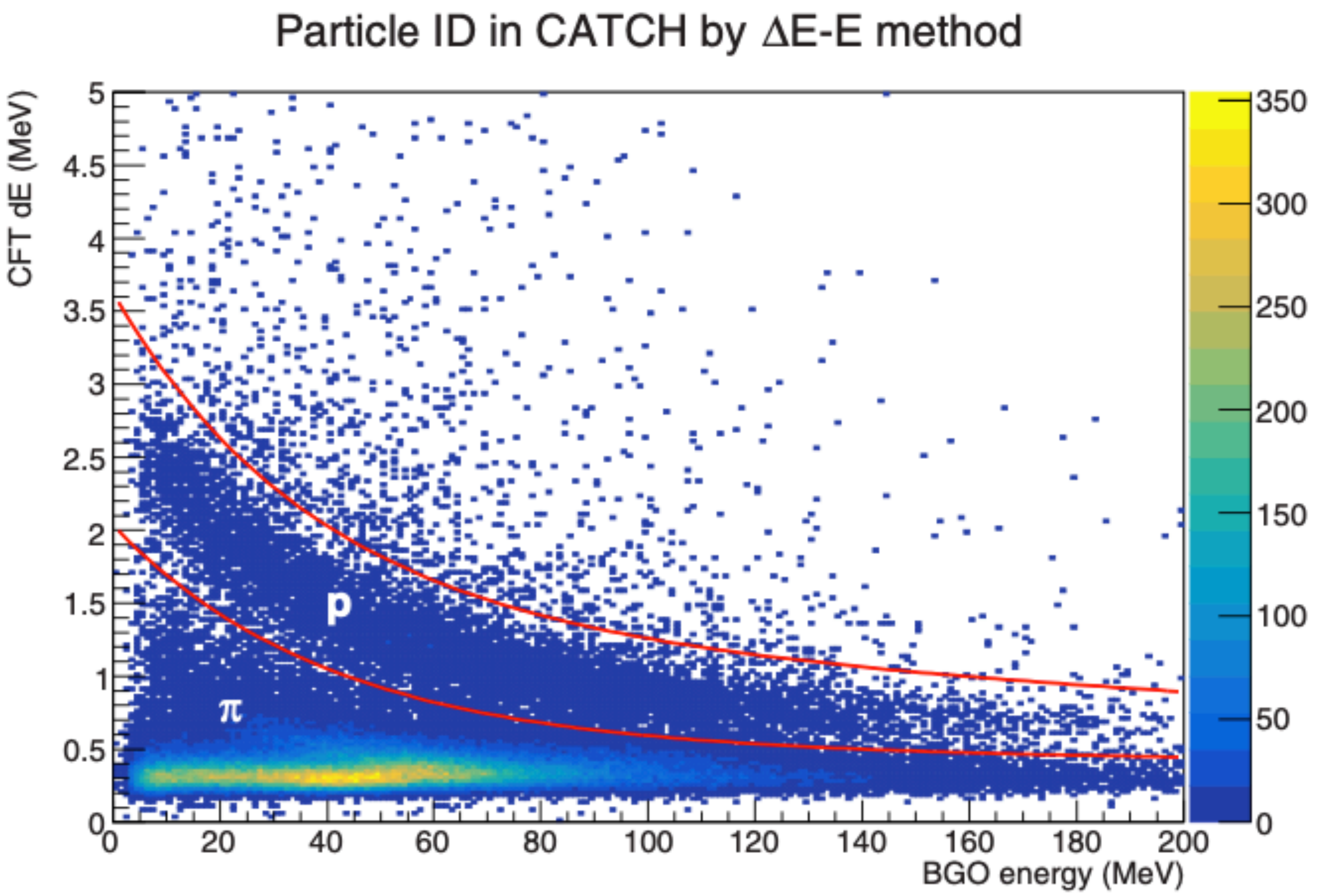

FIG. 8. Correlation between the total energy measured by the BGO and the energy deposit normalized to the unit length in CFT. The two curves show the selection region for the proton. Many of the πs were not stopped in the BGO and penetrated with only a part of the energy deposit.

3. Analysis (3)

vtx_{decay} : Decay point of Λ

A vertex point as the closest point between two tracks of p and π was required to be within 40 mm from the target center.

Closest distance was required less than 5 mm.

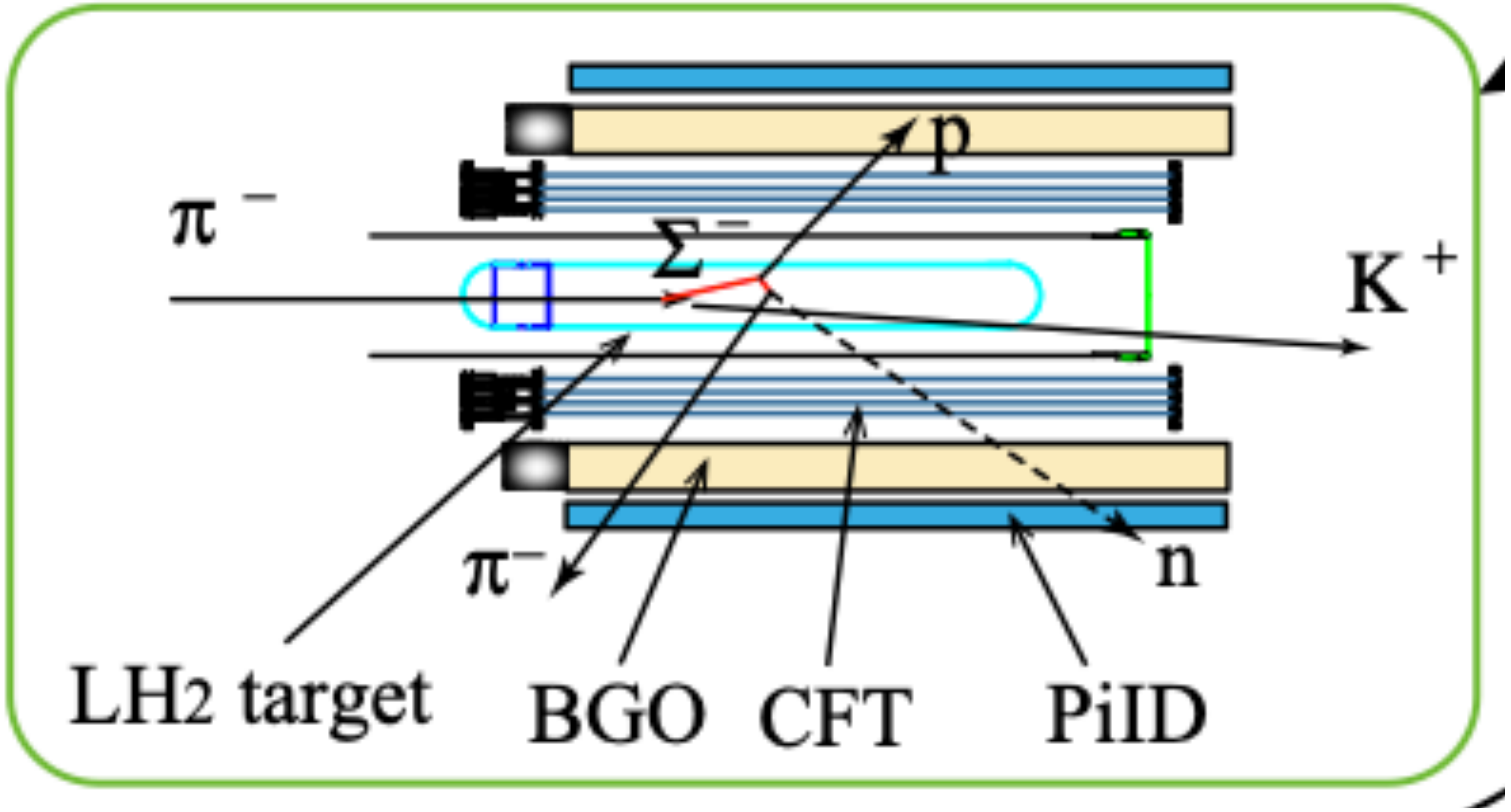

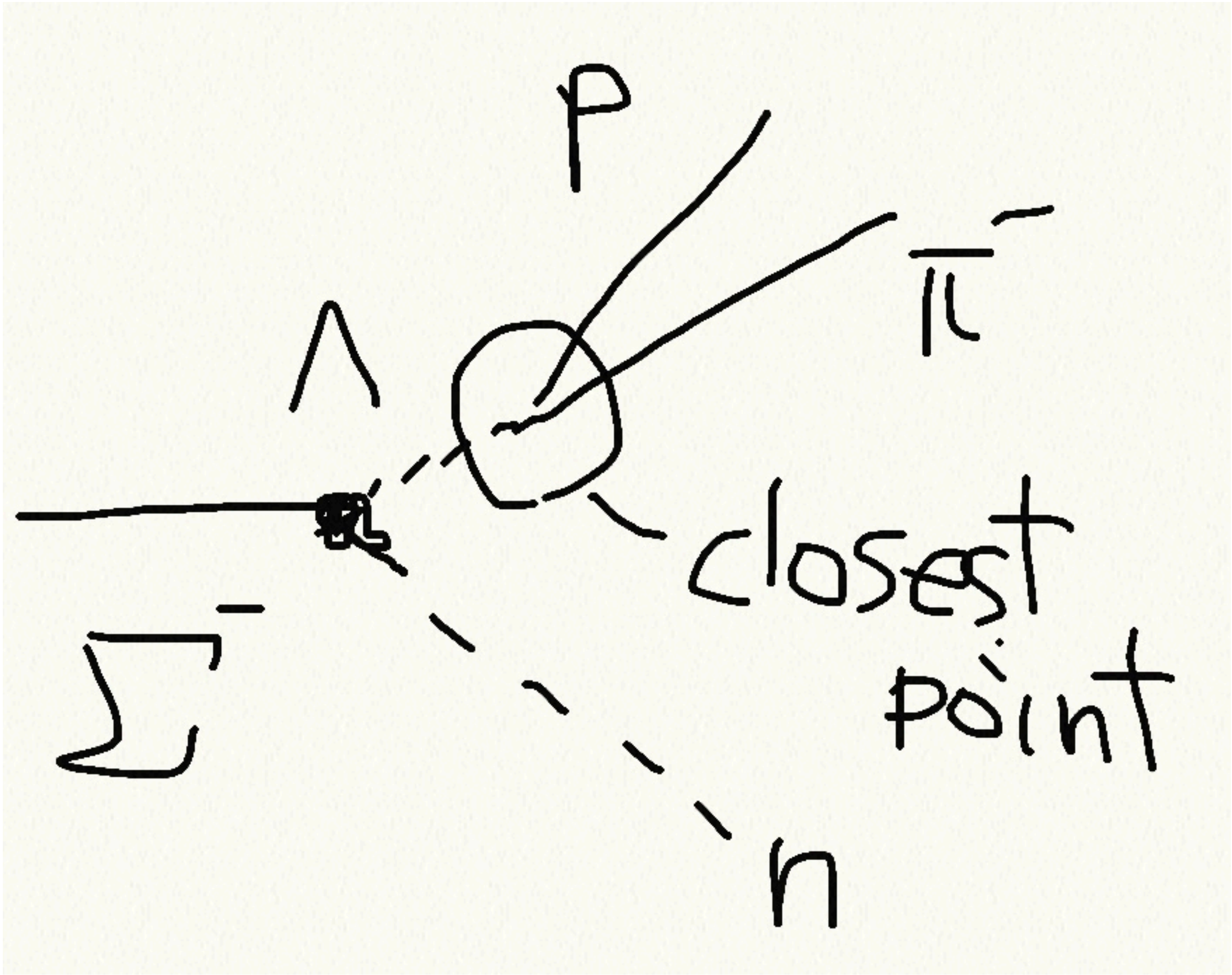

3. Analysis (4)

$p_{\Lambda}^{(\Lambda \to p\pi)}$ (reconstructed with the assmption of the $\Lambda \to p\pi^-$ decay) is cheched to determine whether $p_{\Lambda}^{(\Lambda \to p\pi)}$ is consistent with the $p_{\Lambda}^{(\Sigma p \to \Lambda n)}$ (calculated based on the $\Sigma^- p \to \Lambda n$ kinematics)

$\Delta p_{\Lambda} \equiv p_{\Lambda}^{(\Lambda \to p\pi)} - p_{\Lambda}^{(\Sigma p \to \Lambda n)}$

$0.3 \leq \cos\theta \leq 0.4$ (θ : scattering angle between Σ and Λ)

$470 \leq p_{\Sigma} \leq 550$ MeV/c

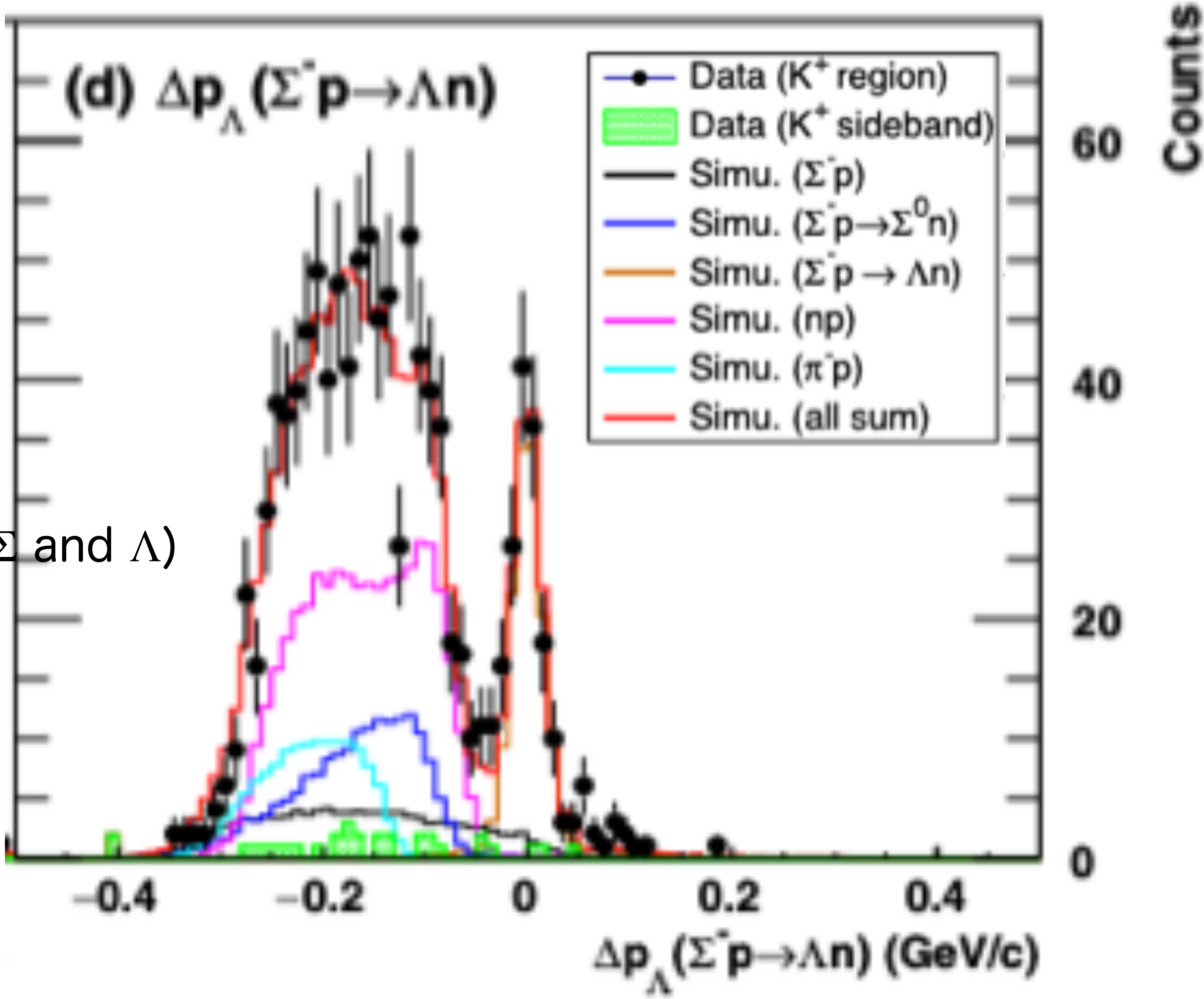

・Peak around Δp_{Λ}=0 —> $\Sigma^- p \to \Lambda n$ events

・Broad structure on the left side
—> other secondary reaction

3. Analysis (5)

$$\frac{d\sigma}{d\Omega} = \frac{\sum_{i_{vtz}} \frac{N_{\text{scat}}(i_{vtz}, \cos\theta)}{\epsilon(i_{vtz}, \cos\theta)}}{\rho N_A L \Delta\Omega}$$

ρ : density, N_A : Avogadro’s number

L : the total flight of length of the Σ^- in LH_2

i_{vtz} represents the index of the z vertex position from -150 mm to 150 mm with an interval of 30 mm. For a scattering angle θ in the c.m. frame and a z vertex position of i_{vtz}, $N_{\text{scat}}(i_{vtz}, \cos\theta)$ and $\epsilon(i_{vtz}, \cos\theta)$ represent the number of $\Sigma^- p \to \Lambda n$ reaction events and the detection efficiency of the CATCH system, respectively. The numerator is the efficiency-corrected number of scattering events. $\Delta\Omega$ represents the solid angle for each scattering angle.

3. Analysis (6)

The number of scattering events was estimated from the $\Delta p_\Lambda(\Sigma^- p \to \Lambda n)$ spectra for each scattering angle,

The error bars and boxes show the statistical and systematic errors, respectively.

The detection efficiency for the $\Sigma^- p \to \Lambda n$ scattering events $[\epsilon(i_{vtz}, \cos\theta)]$ was studied using a realistic Monte Carlo simulation based on the Geant4 package [53], where the realistic angular resolution, the tracking efficiency of CFT, and the realistic energy resolution for BGO were taken into account [10]. The generated data of

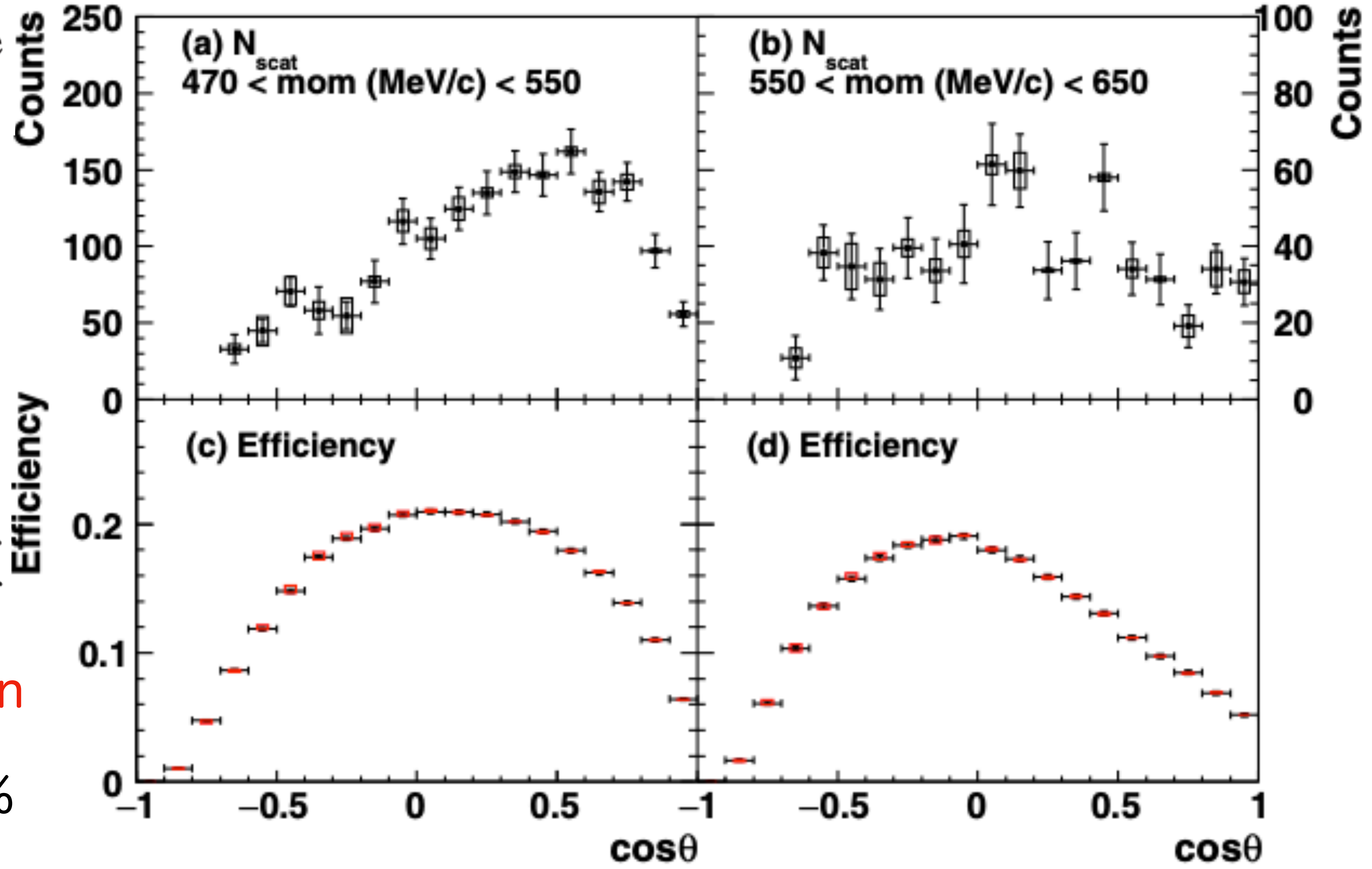

Efficiencies averaged for the z vertex region

Red box : systematic uncertainty 0.5%~3%

In the backward angle, E^p_{kin} from the Λ decay is too small to be detected.

4. Result (1)

- Slightly forward peak structure

- In contrast the $\Sigma^- p$ elastic scattering, sizable contribution exist for backward angular region.

- fss2 (including QCM) and the extended χEFT reproduced the measured data adeqately.

- The Nijmengen models (ESC08c, ESC16) underestimate the forward angular region.

- In higher momentum range, $\frac{d\sigma}{d\Omega}$ becomes flatter in its angular dependence.

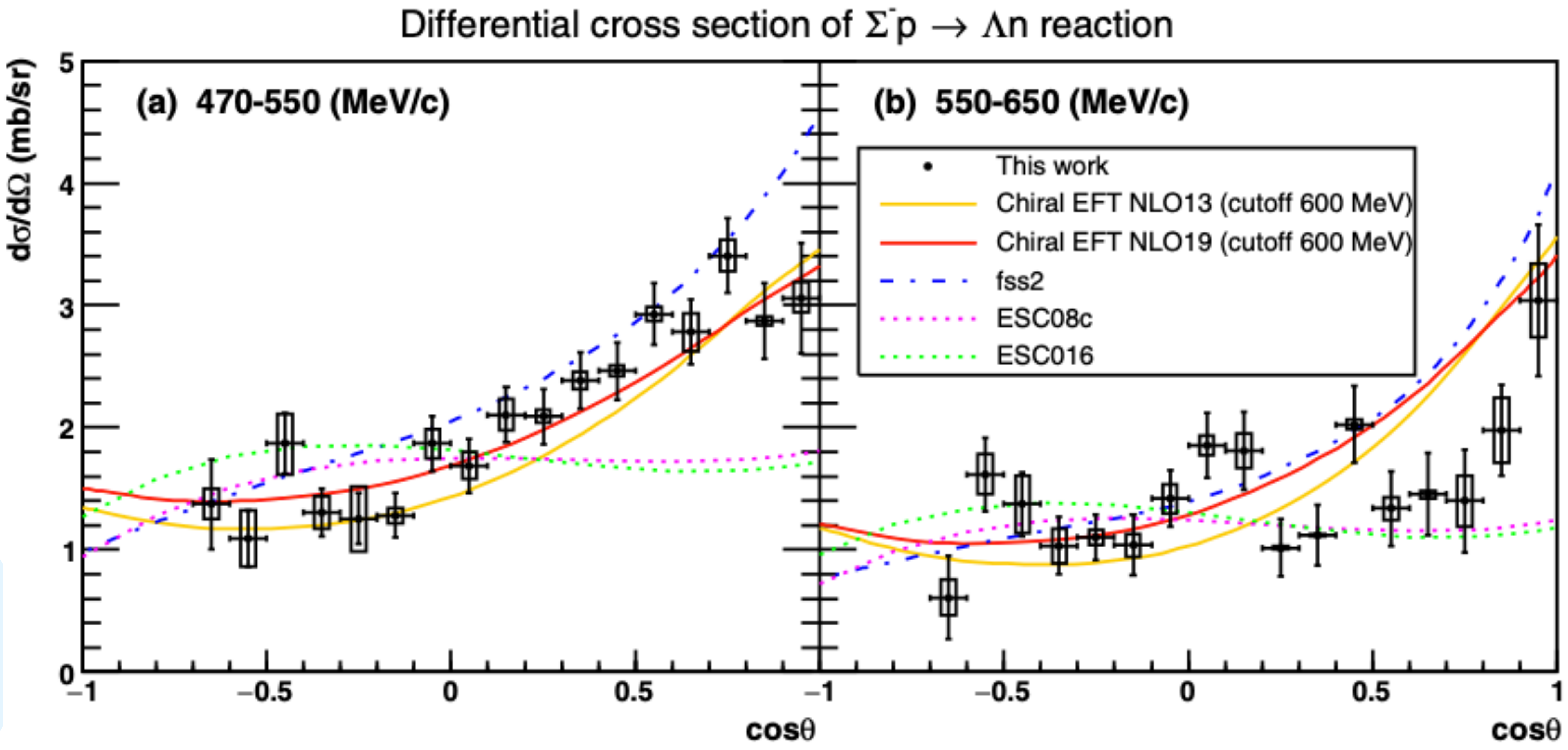

c.f.

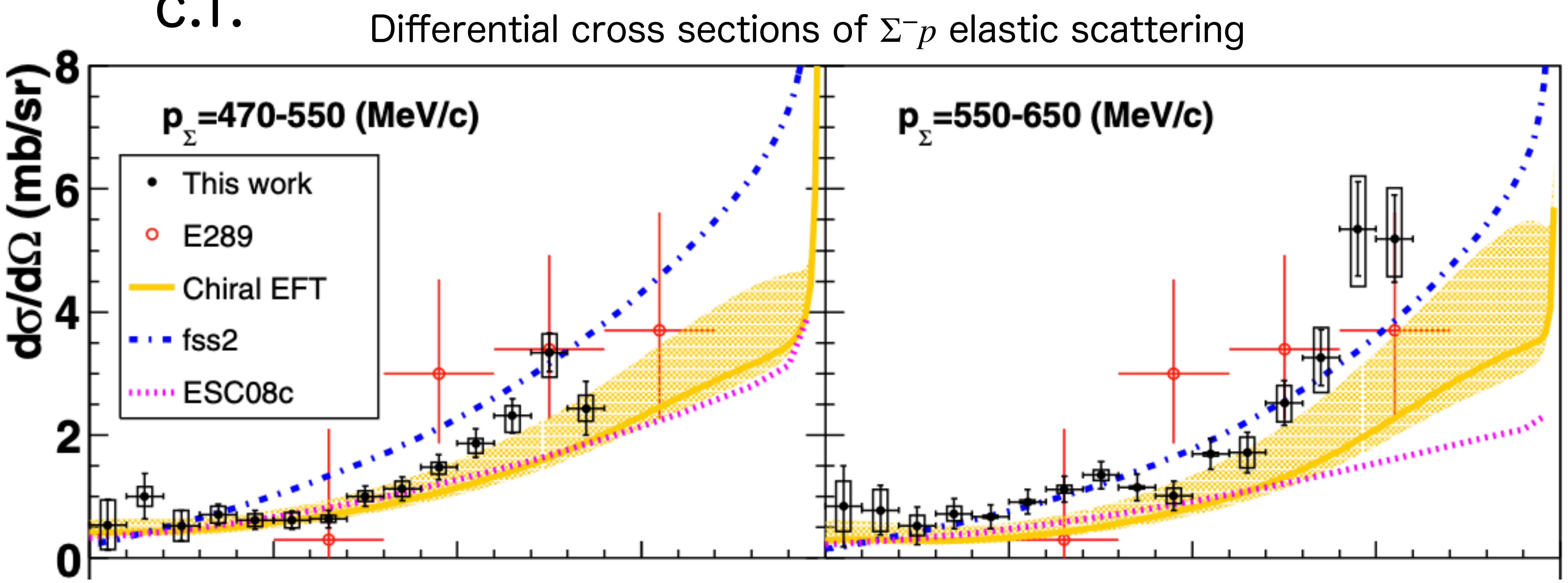

4. Result (2)

The integrated cross sections

22.5 ± 0.68(state)± 0.65(syst) $(470 - 550$ MeV/c)

15.8 ± 0.83(state)± 0.52(syst) $(550 - 650$ MeV/c)

- Past data was measured with a bubble chamber.
- Compared with the past measurement.

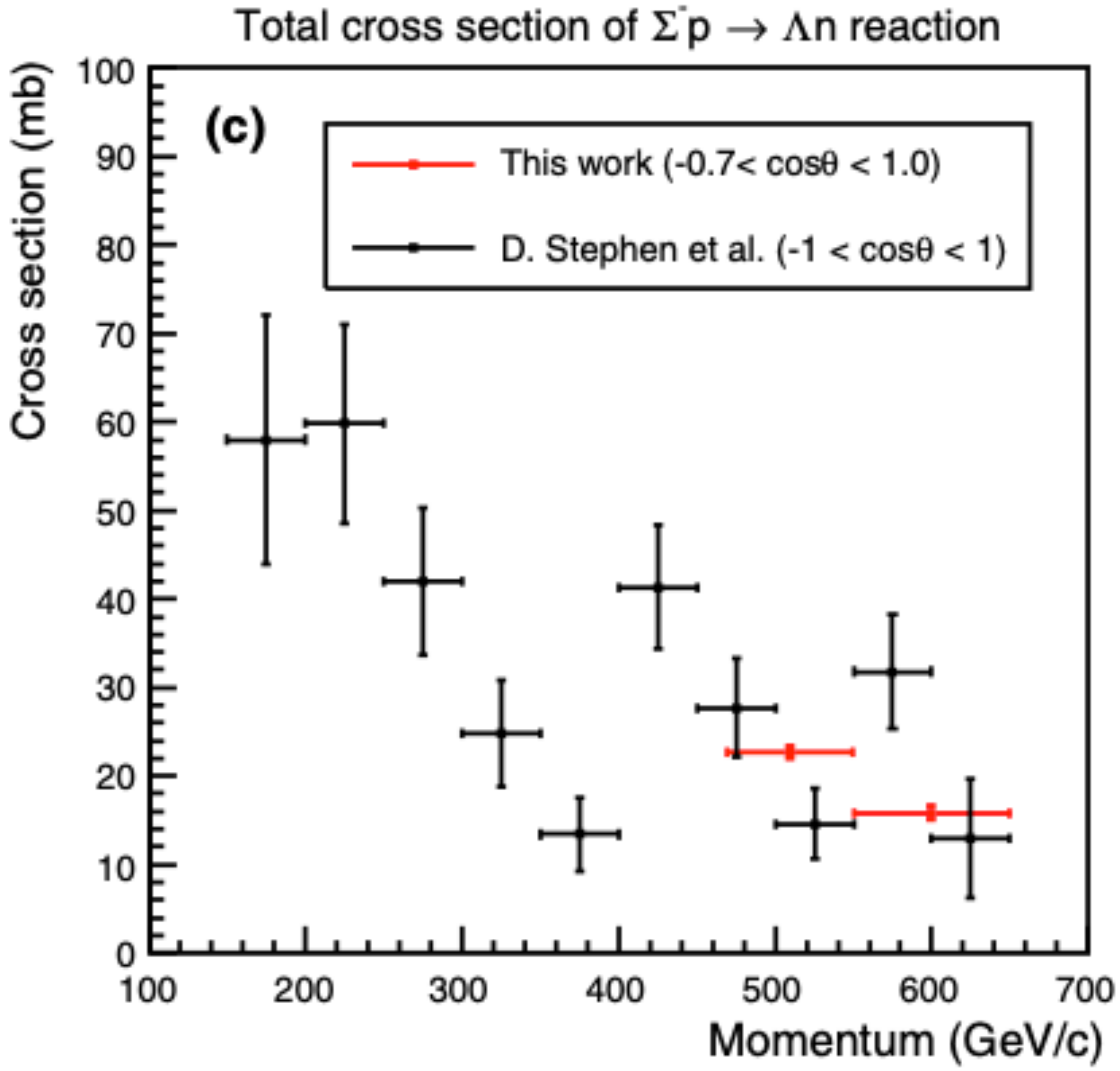

5. Summary

- Successfully mesured $\frac{d\sigma}{d\Omega}$ of the $\Sigma^{-}p \rightarrow \Lambda n$ for the region $470-650$ MeV/c and wide angular region of $-0.7 \leq \cos\theta \leq 1.0$ at J-PARC K1.8 beam line.

- The fss2 and χEFT reproduce both the $\Sigma^{-}p$ elastic scattering and the $\Sigma^{-}p \rightarrow \Lambda n$ reaction.

- The ESC models underestimate $\frac{d\sigma}{d\Omega}$ at the forward angular regions for both channel.

- Integrated cross section were obtained with a drastically improved accuracy.

- The present data and Λp scattering data (in future exp. proposed at J-PARC) will provide new insight into the $\Lambda N-\Sigma N$ coupling.

- These accurate measurements will play an essentioal role in establishing realistic BB interaction model.

Thank you for listening.